Mon. Not. R. Astron. Soc. **000**, 1–6 (2014) Printed 30 April 2014 (MN LATEX style file v2.2)

K2 observations of the pulsating subdwarf B star EQ Piscium: an sdB+dM binary

C. S. Jeffery[1,2] and G. Ramsay[1]
[1] *Armagh Observatory, College Hill, Armagh BT61 9DG, UK*
[2] *School of Physics, Trinity College Dublin, College Green, Dublin 2, Ireland*

arXiv:1404.7470v1 [astro-ph.SR] 29 Apr 2014

30 April 2014

ABSTRACT
K2, the two-wheel mission of the *Kepler* space telescope, observed the pulsating subdwarf B star EQ Psc during engineering tests in 2014 February. In addition to a rich spectrum of g-mode pulsation frequencies, the observations demonstrate a light variation with a period of 19.2 h and a full amplitude of 2%. We suggest that this is due to reflection from a cool companion, making EQ Psc the longest-period member of some 30 binaries comprising a hot subdwarf and a cool dwarf companion (sdB+dM), and hence useful for exploring the common-envelope ejection mechanism in low-mass binaries.

Key words: binaries: close – stars: subdwarfs – stars: oscillations – stars: variables: general – stars: individual: EQ Psc

1 INTRODUCTION

The hot subdwarf EQ Psc (=PB 5450) was one of a number of stars discovered to show long-period pulsations likely to be due to opacity-driven gravity-modes (Green et al. 2003). Both gravity and pressure-mode pulsations are found amongst a significant fraction of hot subdwarfs, and offer the possibility to study the stellar interior using the methods of asteroseismology. During the first two-years of operation of the *Kepler* spacecraft, some twenty pulsating hot subdwarfs were identified in the *Kepler* field and observed for one or more quarters. The majority of these stars are primarily cool V1093 Her (g-mode) variables, one is a hybrid DW Lyn (p-mode + g-mode) variable and one is a low-amplitude V361 Her (p-mode) variable, although very-low amplitude p-modes are detected in a substantial fraction of the *Kepler* V1093 Her variables (Kawaler et al. 2010; Reed et al. 2010).

In addition to pulsation-driven light-variations, subdwarf B stars in binary systems can also show light variations caused by eclipses and/or by reflection from a companion (HW Vir variables) (Menzies & Marang 1986), ellipsoidal deformation in a very short-period binary (*e.g.* KPD 1930+2752) (Billères et al. 2000) and Doppler beaming (*e.g.* 2M 1938+4603) (Barlow et al. 2012). Such phenomena are vital tools for interpreting the fundamental properties, internal structure and evolutionary origin of hot subdwarfs which, by several means, have become nearly-naked core-helium-burning stars (Heber 1986; Han et al. 2002).

Because of the rarity of hot subdwarfs and the significance of light variability for understanding them, it is natural that any such star which falls within a *Kepler* pointing should, if possible, be observed. EQ PSc happened to fall in a field used for a nine-day engineering test at the start of 2014 to verify the stability of operations with two reaction wheels (*K2*) (Howell et al. 2014). In this letter, we report observations which show a 19 h periodic variation, which we interpret as being due to reflection from a cool stellar companion, as well as a rich g-mode pulsation spectrum.

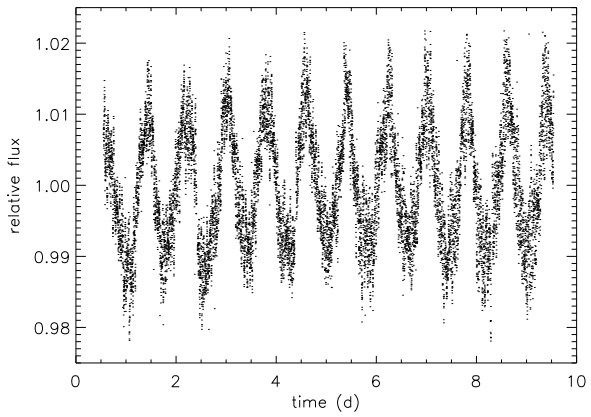

Figure 1. The *K2* light curve for EQ Psc in relative flux units. Times in all figures are given as MJD - 56692.

© 2014 RAS

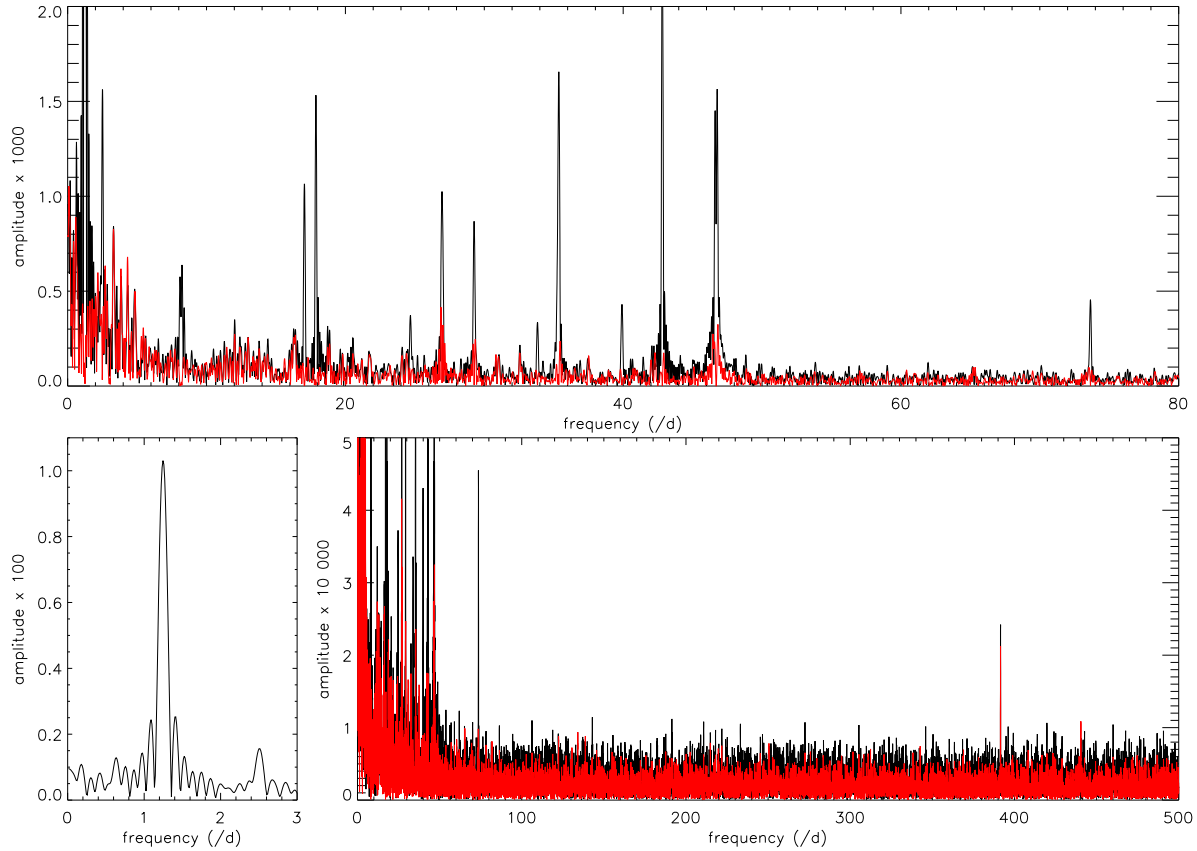

Figure 2. Amplitude spectra obtained from the *K2* light curve of EQ Psc. In all panels, black represents the power spectrum of the data shown in Fig. 1, and red represents the power spectrum of the data pre-whitened by the frequencies and amplitudes shown in Table 1.

Table 1. Frequencies identified in the *K2* power spectrum of EQ PSc.

	f (d^{-1})	P (s)	a (ppt)	ϕ
$f_{\rm orb}$	1.2478	69242	10.218(107)	0.494(02)
$2f_{\rm orb}$	2.4956	34621	1.300(108)	1.240(14)
$f_{\rm L+}$	8.0831	10697	0.569(110)	0.098(31)
$f_{\rm L-}$	8.2256	10512	0.611(110)	0.089(29)
$f_{\rm K}$	17.0468	5085.4	0.986(108)	0.373(17)
$f_{\rm J}$	17.8751	4851.4	1.506(108)	1.235(11)
$f_{\rm I}$	24.6959	3523.3	0.375(108)	0.334(46)
$f_{\rm H}$	26.9578	3232.0	1.073(110)	0.898(16)
$f_{\rm H-}$	27.0933	3216.1	0.321(110)	0.423(54)
$f_{\rm G}$	29.2696	2981.1	0.943(108)	0.286(19)
$f_{\rm F}$	33.8270	2587.3	0.360(108)	0.912(48)
$f_{\rm E+}$	35.2728	2484.8	0.723(111)	0.177(24)
$f_{\rm E}$	35.3638	2478.5	1.601(111)	0.869(11)
$f_{\rm D}$	39.9094	2204.8	0.451(108)	0.393(38)
$f_{\rm C}$	42.8191	2060.6	2.322(108)	0.634(07)
$f_{\rm B+}$	46.6886	1897.2	6.573(381)	0.557(09)
$f_{\rm B-}$	46.7061	1896.6	6.698(381)	0.124(09)
$f_{\rm A}$	73.6477	1246.8	0.424(108)	-0.237(41)

2 *K2* OBSERVATIONS AND DATA REDUCTION

The detector on board *Kepler* is a shutterless photometer using 6 s integrations and a 0.5 s readout. The observations of EQ Psc were made in short cadence (SC) mode, where 9 integrations are summed for an effective 58.8 sec exposure. Observations were carried out in engineering mode from MJD 56692.5411 to 56701.5306 (2014 Feb 4th to Feb 13). The coverage was therefore 8.9 days in duration. During this time interval there were frequent corrections to the spacecraft pointing, with one significant shift occuring on MJD=56694.86 (or 2.3 days into the time series).

A 50×50 pixel array is downloaded from the satellite for each target. To extract a light curve of EQ Psc we used the `PyKe` software (Still & Barclay 2012)[1] which was developed for the *Kepler* mission by the Guest Observer Office. We experimented by extracting data from a series of different combinations of pixels. We found that a mask centered on EQ Psc consisting of 110 pixels gave the optimal results. If a smaller number of pixels are used we find that there are small discontinuities present in the light curve which are the result of small shifts in the position of the stellar profile over the CCD. We also experimented with subtracting the background (which increased in a nearly linear fashion over the course of the observations) in different ways. We found

[1] http://keplergo.arc.nasa.gov/PyKE.shtml

that using the median value of each time point to represent the background gave the best results. Finally we removed time points which were not flagged `'SAP_QUALITY==0'` (for instance during times of enhanced solar activity). The extracted and reduced light curve is shown in Fig. 1

3 LIGHT CURVE AND FREQUENCY ANALYSIS

The *K2* light curve for EQ PSc shows a strong modulation with an amplitude of about two per cent (0.022 mag) and a period close to 0.8 d (Fig. 1). Closer inspection shows additional variability on a timescale of half an hour with an amplitude of around one per cent.

The periodic content of the light curve was investigated using a classical power spectrum analysis. An idea of the window function can be obtained from the lower-left panel in Fig. 2. For a continuous run lasting 9 d, the nominal frequency resolution is $0.22\,\mathrm{d}^{-1}$. Peaks in the power spectrum were identified in order of descending power, amplitudes and phases associated with each peak were measured using a multi-sine fit to the light curve, the light curve was pre-whitened by this fit, a new power spectrum was computed, the next-highest peaks were identified and added to the frequency table, and the cycle was iterated.

A provisional list of frequencies in cycles per day, periods in seconds, semi-amplitudes in parts per thousand (ppt[2]), and phases representing the *K2* lightcurve of EQ Psc is presented in Table 1. Phases refer to a zero-point at MJD 56692.0 and are given in cycles. Errors are shown in parentheses. The multi-sine fit constructed from the data in this table is illustrated in Fig. 3. Frequencies have been labelled in alphabetical order of increasing period.

Several low-frequency peaks were excluded from this analysis; with the exception of the dominant peak at $1.248\,\mathrm{d}^{-1}$, its first harmonic and their aliases, the power spectrum is dominated by red noise at $f < 5\,\mathrm{d}^{-1}$. At $f > 100\,\mathrm{d}^{-1}$, the power spectrum has the characteristics of all *Kepler* SC data (Baran 2013), including a peak at $\approx 390\,\mathrm{d}^{-1}$ and a picket fence of low-amplitude peaks just visible in the lower-right panel of Fig. 2. None of these were considered to have a stellar origin. The highest-frequency signal f_A ($P_\mathrm{A} \approx 21$ m) is isolated from than the main group of g-mode frequencies. It may be a *K2* artefact. There is a variable artefact at around $31 - 32\,\mathrm{d}^{-1}$ (Baran 2013), but this is well clear of f_F. f_K is close to a known broad feature at $16.98\,\mathrm{d}^{-1}$ in *Kepler* SC data.

There remain a number of significant peaks in the power spectrum after subtracting the 18-frequency solution shown here. These are all low-amplitude partners to much stronger peaks; examples include the base of the doublet at $46.7\,\mathrm{d}^{-1}$ and peaks at 27.1 and $29.3\,\mathrm{d}^{-1}$ Given the frequency resolution of our data, these may not be real. This is demonstrated by the large amplitudes in the fit to the $46.7\,\mathrm{d}^{-1}$ doublet, which do not reflect the height of the peaks in the power spectrum. The clue is in the phases, which are almost half a cycle different at the start of the run. Since the beat period between these two frequencies is some 57 days, the oscillations in the model are almost in anti-phase for the duration of the observations. As for other V1093 Her variables, it will require a much longer observing run to fully resolve the g-mode oscillations in this star.

In contrast to the sixteen or more pulsating sdB stars previously observed with *Kepler* (Østensen et al. 2011; Baran et al. 2011), the frequency resolution of the current data limits the information that can be extracted for asteroseismic analysis. It would be useful, for example, to identify series and multiplets with large and small period spacings, respectively, but this is not possible here. Where two frequencies in Table 1 are identified with a spacing less than the nominal experimental resolution ($0.22\,\mathrm{d}^{-1}$), they have been marked B–, B+, etc. If one component is much stronger than the near-neighbour, the suffix is omitted from the strongest component.

Frequencies $f_\mathrm{B} - f_\mathrm{L}$, corresponding to periods in the range 1800 - 11000 s, are typical of periods commonly seen in V1093 Her variables (Østensen et al. 2011; Baran et al. 2011). Green et al. (2003) show 3 h of R-band photometry for EQ PSc, which demonstrates variability on timescales of $\approx$ 30 minutes. This corresponds well with the doublet $f_{\mathrm{B}-,\mathrm{B}+}$. Despite the nominal resolution, this peak is clearly resolved in our power spectrum (Fig, 2) with a separation $\Delta f = 0.018\,\mathrm{d}^{-1}$. We conclude that frequencies $f_\mathrm{B} - f_\mathrm{L}$ are associated with g-mode pulsations in EQ Psc.

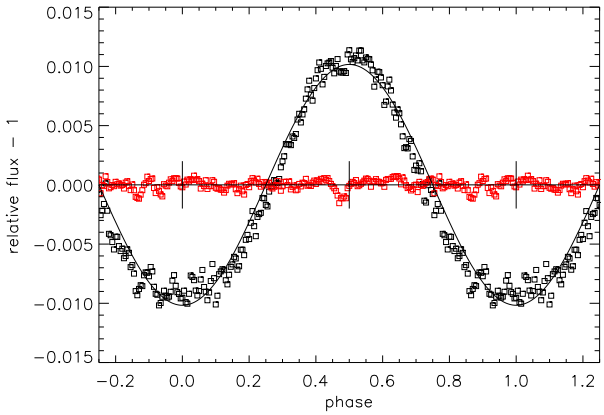

Figure 4. The *K2* light curve for EQ Psc binned ($\delta\phi = 0.005$, black squares: relative flux - 1) and the residual light curve (red squares) folded on the orbital frequency. The first element of the fit (Table 1) is shown as a solid line. There is no evidence for an eclipse at either phase 0.0 (primary) or 0.5 (secondary).

4 ORBITAL REFLECTION IN A SDB+DM BINARY

EP Psc shows a strong periodic signal at 0.801 d (19.2 h) with a full (peak-to-peak) amplitude > 2% of total light. The *K2* data folded on this period are shown in Fig. 4. The same data pre-whitened by the Table 1 solution and filtered to remove low-frequency (red) noise ($f < 3\,\mathrm{d}^{-1}$) are shown in the same figure.

The presence of an harmonic shows that this is not perfectly sinusoidal. Indeed, the roughly quarter-cycle phase

[2] Also referred to as *milli-modulation intensity* units, or mmi.

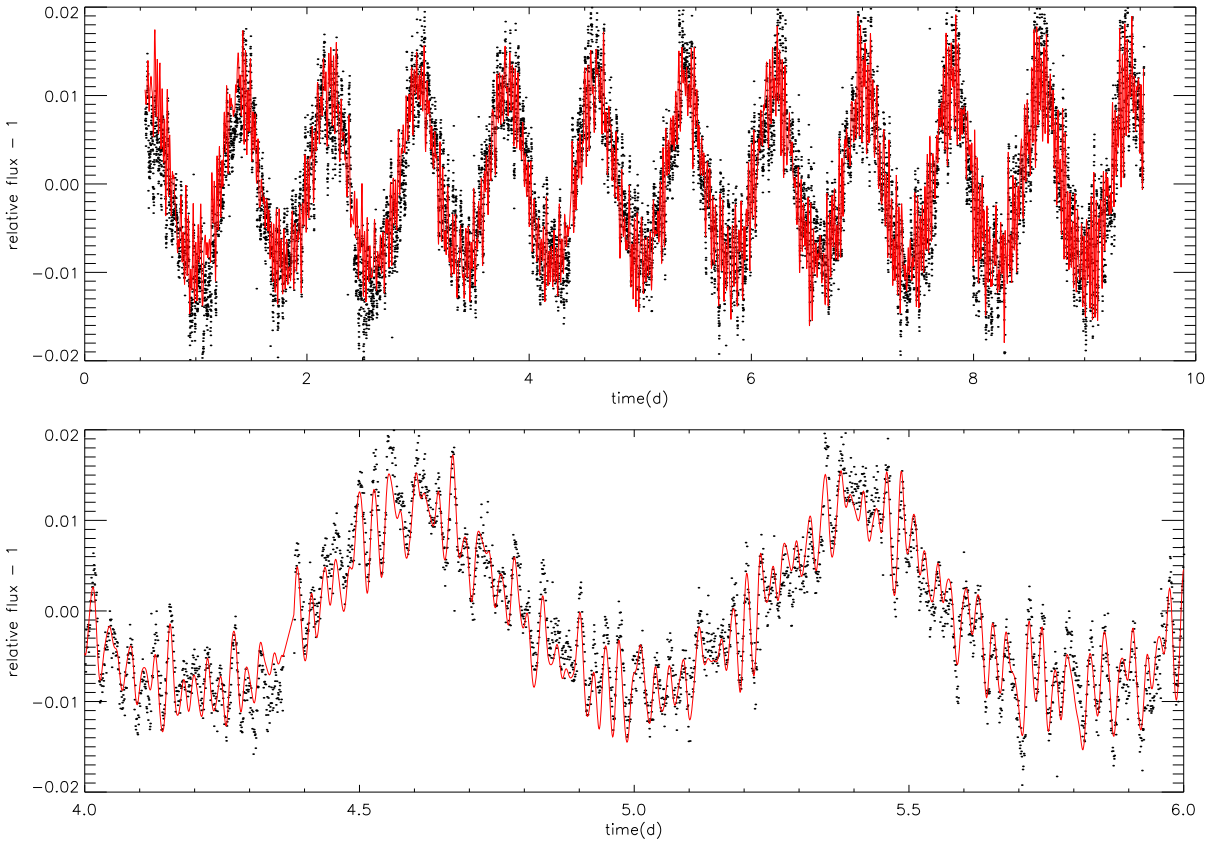

Figure 3. The adopted fit to the *K2* light curve for EQ Psc shown in Fig. 1. Black dots are the *K2* observations. The solid red curve shows the solution represented in Table 1.

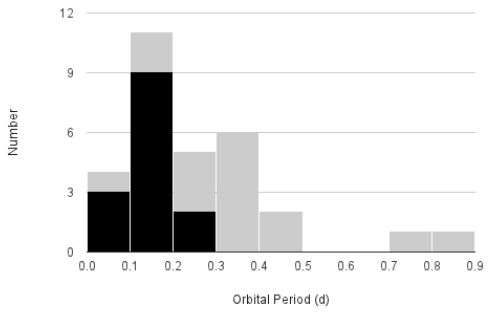

Figure 5. The orbital-period distribution for known sdB+dM binaries, distinguishing eclipsing (HW Vir: black) and non-eclipsing (grey) systems.

difference between the orbital harmonics flattens the minimum and sharpens the maximum. The lightcurve thus resembles those of hot subdwarf + M-dwarf (sdB+dM) binaries in which the heated surface of the M-dwarf facing the hot subdwarf reradiates (reflects) the incident energy. Fourteen sdB+dM binaries with periods in the range 0.069 – 0.261 d show such a reflection effect and also primary and secondary eclipses: these are true HW Vir-type sytems. Fifteen sdB+dM binaries with periods in the range 0.076 – 0.75 d show a reflection effect alone with amplitudes ranging up to 0.1 magnitudes. The prototype is XY Sex (Maxted et al. 2002). The longest-period system before EQ Psc was JL 82 (0.75 d) (Koen 2009).

Since the 0.801 d period is longer and the amplitude much larger than observed in any known g-mode in a pulsating sdB star, pulsation would seem to be a unsatisfactory explanation. Ellipsoidal deformation of the hot star due to rotation and tidal effects can be ruled out because the period is too long (by a factor 10) to account for the amplitude observed. Moreover, an ellipsoidal variation would have twice the period measured, with minima of unequal depth. We conclude that reflection from an M-dwarf or otherwise unseen companion is the most likely explanation for the 0.801 d period in EQ Psc. Confirmation would make EQ Psc the longest-period sdB+dM binary known to date.

In their paper reporting g-mode pulsations in EQ Psc, Green et al. (2003) write "...we did find three low-amplitude variables with periods of several hours or more. Two are sdB stars exhibiting apparent reflection effects, having appropriately phased sinusoidal light curves the same length as their orbital periods ($\sim$ 6 and 12 hr)." The 19.2 h modulation would have been difficult to identify from the 3 h photometry reported for EQ Psc, so its omission at that time is understandable. During the preparation of this letter, the authors have been made aware, however, that subsequent ground-based photometry by Green et al. does show evi-

dence for a low-amplitude reflection effect (Green, Østensen, priv. comm.).

Figure 4 shows no evidence for a primary eclipse, neither in the total flux, nor in the residual flux. A dip just before the expected position of secondary eclipes is consistent with being noise. Geometric considerations alone imply that longer-period sdB+dM binaries are less likely to eclipse, as indicated by the period distributions of eclipsing and non-eclipsing systems (Fig. 5[3]).

In crude terms, the amplitude of the reflection effect is a function of orbital separation $1/a$, cool dwarf diameter $r_{\rm dM}$ and orbital inclination i. Assuming that both components are typical of other sdB+dM binaries. the orbital period indicates a separation $a \approx 3.0 \pm 0.2\,{\rm R}_\odot$, where the uncertainty indicates the spread in the period-separation relation for shorter-period systems. Assuming representative radii of 0.17 $\rm R_\odot$ for both stars (Almeida et al. 2012), we deduce a maximum inclination $i \lesssim 84^\circ$ to avoid eclipses.

The study of long-period sdB+dM binaries is important for stellar evolution theory and, in particular, for understanding the common-envelope ejection process. sdB+dM binaries are believed to originate in a system where an expanding red giant engulfs a low-mass main-sequence companion shortly before core helium ignition (Han et al. 2002). The spiral-in of the M dwarf leads to heating and ejection of the common-envelope surrounding the two stars. The final separation of the components is indicative of the amount of orbital binding energy required to remove the red-giant envelope. In the case of EQ Psc, the long period may be the result of a wider-than-typical orbital separation, and possibly linked with a higher-than-typical mass for the M dwarf.

5 CONCLUSION

Observations obtained during an engineering run with *K2* in 2014 February have shown that thruster-assisted, two wheel operation, is sufficiently stable to obtain stellar photometry with high precision. The known pulsating subdwarf B star EQ Psc has been demonstrated to show a 2% light modulation with a period of 19.2 h. It is argued that this is most likely due to reflection of light from the hot subdwarf by a cool binary companion; an M dwarf is likely. The light curve also contains a rich spectrum of higher frequency oscillations with periods in the range 1800 - 10 000 s. Most of these are likely to be associated with g-mode pulsations, as identified by Green et al. (2003). Spectroscopic studies of the binary orbit and of the hot star atmosphere are desirable. Opportunities to explore the g-mode pulsation spectrum in more detail should be pursued.

[3] Periods for eclipsing (HW Vir) systems shown in Fig. 5 were taken from: Schaffenroth et al. (2014) (SDSS J1622+4730: 0.0697 d), Drechsel et al. (2001) (HS 0705+6700: 0.096 d), Geier et al. (2011) (SDSS J0820+0008: 0.096 d), Kilkenny et al. (1998) (NY Vir: 0.101 d), Wils et al. (2007) (NSVS 14256825: 0.1104 d), Østensen et al. (2007) (HS 2231+2441: 0.1106 d), Menzies & Marang (1986) (HW Vir: 0.1168 d), Barlow et al. (2013) (EC 10246-2707: 0.1185 d), Polubek et al. (2007) (OGLE BUL-SC16 335: 0.1251 d), Østensen et al. (2010) (2M 1938+4603: 0.126 d), Schaffenroth et al. (2013) (ASAS 102322-3737.0: 0.1393 d), For et al. (2010) (2M 1533+3759: 0.162 d), Pribulla et al. (2013) (FBS 0747+725: 0.21 d) and Kilkenny et al. (1978) (AA Dor: 0.261 d). Periods for non-eclipsing (XY Sex) systems are from: Maxted et al. (2002) (XY Sex: 0.073 d), Kupfer et al. (2013) (UVEX J0328+5035: 0.11017 d), Heber et al. (2004) (HS 2333+3927: 0.1718 d), Morales-Rueda et al. (2003) (PG 1329+159: 0.2497 d), Østensen et al. (2013) (FBS 0117+396: 0.252 d), For et al. (2008) (2M 1926+3720: 0.2923 d), Geier et al. (2014) (HS 2043+0615: 0.3016 d), Green et al. (2004) (PG 1438-029: 0.3358 d), Latour et al. (2013) (Feige 48: 0.3438 d), Kawaler et al. (2010) (KIC 11179657: 0.3944 d and KIC 2991403: 0.4431 d), Koen et al. (1999) (V1405 Ori: 0.398 d), Pablo et al. (2011) (B4 NGC6791: 0.3985 d), Koen (2007) (HE 0230-4323: 0.4515 d), Koen (2009) (JL 82: 0.75 d) and this paper (EQ Psc: 0.801 d).

ACKNOWLEDGMENTS

This paper includes data collected by the Kepler spacecraft using thruster-assisted, two wheel operation. Funding for the Kepler spacecraft is provided by the NASA Science Mission Directorate. The data were obtained through the Mikulski Archive for Space Telescopes (MAST). STScI is operated by the Association of Universities for Research in Astronomy, Inc., under NASA contract NAS5-26555. Support for MAST for non-HST data is provided by the NASA Office of Space Science via grant NNX09AF08G and by other grants and contracts. This work made use of PyKE, a software package for the reduction and analysis of Kepler data. This open source software project is developed and distributed by the NASA Kepler Guest Observer Office. We thank Tom Barclay, Martin Still and Steve Howell for useful advice. We thank the referee for prompt and constructive comments. Armagh Observatory is supported by direct grant from the Northern Ireland Department of Culture, Arts and Leisure.

REFERENCES

Almeida L. A., Jablonski F., Tello J., Rodrigues C. V., 2012, MNRAS, 423, 478
Baran A. S., 2013, Acta Astron., 63, 203
Baran A. S., Kawaler S. D., Reed M. D., et al., 2011, MNRAS, 414, 2871
Barlow B. N., Kilkenny D., Drechsel H., et al., 2013, MNRAS, 430, 22
Barlow B. N., Wade R. A., Liss S. E., 2012, ApJ, 753, 101
Billères M., Fontaine G., Brassard P., Charpinet S., Liebert J., Saffer R. A., 2000, ApJ, 530, 441
Drechsel H., Heber U., Napiwotzki R., Østensen R., Solheim J.-E., Johannessen F., Schuh S. L., Deetjen J., Zola S., 2001, A&A, 379, 893
For B.-Q., Edelmann H., Green E. M., Drechsel H., Nesslinger S., Fontaine G., 2008, in Heber U., Jeffery C. S., Napiwotzki R., eds, Hot Subdwarf Stars and Related Objects, ASPCS 392, 203
For B.-Q., Green E. M., Fontaine G., et al. 2010, ApJ, 708, 253
Geier S., Hirsch H., Tillich A., et al., 2011, A&A, 530, A28
Geier S., Østensen R. H., Heber U., et al., 2014, A&A, 562, 95
Green E. M., Fontaine G., Reed M. D., et al., 2003, ApJ, 583, L31

Green E. M., For B., Hyde E. A., et al., 2004, Ap&SS, 291, 267
Han Z., Podsiadlowski P., Maxted P. F. L., Marsh T. R., Ivanova N., 2002, MNRAS, 336, 449
Heber U., 1986, A&A, 155, 33
Heber U., Drechsel H., Østensen R., et al., 2004, A&A, 420, 251
Howell S. B., Sobeck C., Haas M., 2014, arXiv:1402.5163
Kawaler S. D., Reed M. D., Quint A. C., et al., 2010, MNRAS, 409, 1487
Kilkenny D., Hilditch R. W., Penfold J. E., 1978, MNRAS, 183, 523
Kilkenny D., O'Donoghue D., Koen C., Lynas-Gray A. E., van Wyk F., 1998, MNRAS, 296, 329
Koen C., 2007, MNRAS, 377, 1275
Koen C., 2009, MNRAS, 395, 979
Koen C., O'Donoghue D., Kilkenny D., Stobie R. S., Saffer R. A., 1999, MNRAS, 306, 213
Kupfer T., Geier S., McLeod A. F., et al., 2013, ArXiv:1308.2447
Latour M., Fontaine G., Green E. M., 2013, ArXiv:1307.6112
Maxted P. F. L., Marsh T. R., Heber U., Morales-Rueda L., North R. C., Lawson W. A., 2002, MNRAS, 333, 231
Maxted P. F. L., Marsh T. R., Moran C. K. J., 2002, MNRAS, 332, 745
Menzies J. W., Marang F., 1986, in Hearnshaw J. B., Cottrell P. L., eds, Instrumentation and Research Programmes for Small Telescopes, IAU Symposium, Vol. 118, p. 305
Morales-Rueda L., Maxted P. F. L., Marsh T. R., North R. C., Heber U., 2003, MNRAS, 338, 752
Østensen R., Oreiro R., Drechsel H., Heber U., Baran A., Pigulski A., 2007, in Napiwotzki R., Burleigh M. R., eds, 15th European Workshop on White Dwarfs, ASPCS 372, 483
Østensen R. H., Geier S., Schaffenroth V., et al. 2013, A&A, 559, 35
Østensen R. H., Silvotti R., Charpinet S., et al., 2011, MNRAS, 414, 2860
Østensen R. H., Silvotti R., Charpinet S., Oreiro R., Handler G., Green E. M., Bloemen S., Heber U., et al. 2010, MNRAS, 409, 1470
Pablo H., Kawaler S. D., Green E. M., 2011, ApJ, 740, L47
Polubek G., Pigulski A., Baran A., Udalski A., 2007, in Napiwotzki R., Burleigh M. R., eds, 15th European Workshop on White Dwarfs, ASPCS 372, 487
Pribulla T., Dimitrov D., Kjurkchieva D., et al., 2013, IBVS, 6067, 1
Reed M. D., Kawaler S. D., Østensen R. H., et al., 2010, MNRAS, 409, 1496
Schaffenroth V., Geier S., Drechsel H., Heber U., Wils P., Østensen R. H., Maxted P. F. L., di Scala G., 2013, A&A, 553, A18
Schaffenroth V., Geier S., Heber U., Kupfer T., Ziegerer E., Heuser C., Classen L., Cordes O., , 2014, ArXiV:1402.5263
Still M., Barclay T., 2012, Astrophysics Source Code Library, record 1208.004, (http://adsabs.harvard.edu/abs/2012ascl.soft08004S)
Wils P., di Scala G., Otero S. A., 2007, IBVS, 5800, 1